Scheme I. Potential Metabolic Pathways between Ornithine and Hyoscyamine

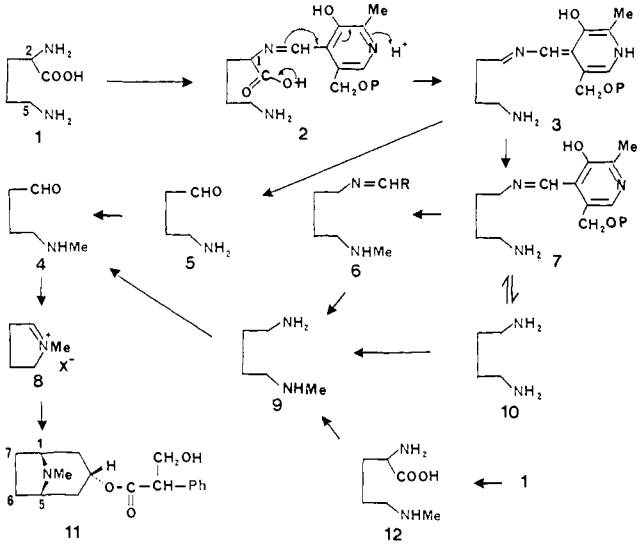

undergoes decaboxylation as illustrated to yield **3**. A tautomeric shift then affords the Schiff base of putrescine and pyridoxal phosphate (**7**). It is then proposed that this Schiff base undergoes N-methylation to yield **6**. Hydrolysis of this compound yields N-methylputrescine (**9**). Oxidation of **9** catalyzed by the enzyme *N*-methylputrescine oxidase yields 4-(methylamino)butanal (**4**). The cyclized form of this amino aldehyde is the 1-methyl-Δ^1-pyrrolinium salt (**8**), the generally accepted precursor of the tropane skeleton.[10,11] This pathway, as described, will maintain the integrity of C-2 and C-5 of the initial ornithine and will result in unsymmetrical labeling of the tropane nucleus in hyoscyamine derived from [2-^{14}C]ornithine. In support of this pathway *N*-methylputrescine (**9**) has been established as a precursor of hyoscyamine and scopolamine (the 6,7-epoxide of **11**).[12] To explain the symmetrical labeling reported in the present article we propose that the Schiff base **7** undergoes a ready reversible hydrolysis to free putrescine (**10**) before methylation takes place. An alternative route in *Hyoscyamus albus* would be methylation of this free putrescine to *N*-methylputrescine. Indeed the enzyme putrescine-*N*-methyltransferase has been found in *H. albus* root cultures.[13] High levels of radioactivity were also found in putrescine and *N*-methylputrescine after a short (4 h) feeding of [5-^{14}C]ornithine to *H. albus* root culture.[13]

Another explanation of our results was suggested by a referee. It was proposed that the Schiff base **3** undergoes hydrolysis to 4-aminobutanal (**5**) which is then methylated to 4-(methylamino)butanal (**4**). This would be the pathway operating in *Datura*. The incorporation of *N*-methylputrescine observed in *Datura*[12] could be explained by proposing a transamination of this amine to the 4-(methylamino)butanal.

We formerly rationalized the unsymmetrical incorporation of ornithine into hyoscyamine by propsing the intermediate formation of δ-*N*-methylornithine (**12**) which then underwent decarboxylation to yield *N*-methylputrescine. This amino acid was indeed incorporated unsymmetrically into hyoscyamine.[14] It was also detected (by trapping with the unlabeled amino acid) from *Atropa belladonna* plants which had been fed [5-^{14}C]ornithine.[15] However, we have been unable to detect this amino acid in *Datura* species. In *H. albus*, insignificant radioactivity was detected in δ-*N*-methylornithine (added in a trapping experiment) in root cultures which had been fed [5-^{14}C]ornithine. We currently regard δ-*N*-methylornithine as an unnatural compound, its decarboxylation to *N*-methylputrescine being an aberrant reaction. In tobacco this is indeed the case.[16] [2-^{14}C]-δ-*N*-Methylornithine labeled the pyrrolidine ring of nicotine unsymmetrically, whereas [2-^{14}C]ornithine labels the ring symmetrically via free putrescine.[16]

In conclusion, it is clear that the conversion of ornithine to the 1-methyl-Δ^1-pyrrolinium salt (**8**), a precursor of hyoscyamine, can proceed by two pathways, one of which (in *Datura*) cannot involve free putrescine.[17]

Acknowledgment. This work was supported by a grant from the Ministry of Education, Science and Culture of Japan (to Y.Y.) and research grants (to E.L.) from the National Institutes of Health (GM-13246) and the National Science Foundation (CHE-8620345).

Supplementary Material Available: Full details of the modified degradation scheme of hyoscyamine with the specific activities of the degradation products (4 pages). Ordering information given on any current masthead page. These data will also be provided with requests for reprints.

(9) Hashimoto, T.; Yukimune, Y.; Yamada, Y. *J. Plant Physiol.* **1986**, *124*, 61.
(10) Leete, E. *Planta Med.* **1979**, *36*, 97.
(11) Lounasmaa, M. In *The Alkaloids*; Brossi, A., Ed.; Academis Press: 1988; Vol. 33, p 1.
(12) (a) Liebisch, H. W.; Maier, W.; Schütte, H. R. *Tetrahedron Lett.* **1966**, 4079. (b) Leete, E.; McDonell, J. A. *J. Am. Chem. Soc.* **1981**, *103*, 658.
(13) Hashimoto, T.; Yukimune, Y.; Yamada, Y. *Planta*, in press.
(14) (a) Ahmad, A.; Leete, E. *Phytochemistry* **1970**, *9*, 2341. (b) Baralle, F. E.; Gros, E. G. *Chem. Commun.* **1969**, 721.
(15) Hedges, S. H.; Herbert, R. B. *Phytochemistry* **1981**, *20*, 2064.
(16) Gilbertson, T. J.; Leete, E. *J. Am. Chem. Soc.* **1967**, *89*, 7085.
(17) When [1,4-^{14}C]putrescine was fed to *Datura* species, specific incorporation of radioactivity into the C-1 and C-5 positions of hyoscyamine did occur.[18] However, this is considered to be the result of nonspecific enzymes converting the putrescine to intermediates on the "normal" biosynthetic pathway.
(18) (a) Kaczkowski, J.; Marion, L. *Can. J. Chem.* **1963**, *41*, 2651. (b) Leete, E.; Louden, M. C. L. *Chem. and Ind. (London)* **1963**, 1725. (c) Liebisch, H. W.; Schütte, H. R.; Mothes, K. *Liebigs Annalen* **1963**, 668, 139.

Intervalence Enhanced Raman Scattering from $(NC)_5Ru$-CN-$Ru(NH_3)_5^-$. A Mode-by-Mode Assessment of the Franck-Condon Barrier to Intramolecular Electron Transfer

Stephen K. Doorn and Joseph T. Hupp*

Department of Chemistry, Northwestern University Evanston, Illinois 60208

Received September 21, 1988

A key issue in both inter- and intramolecular electron-transfer kinetics is the assessment of vibrational (Franck-Condon) barriers. These barriers arise from redox-induced differences between initial- and final-state normal coordinates or bond lengths. In favorable cases these differences can be determined from X-ray measurements (either EXAFS or X-ray crystal structures) obtained for different oxidation states, and when combined with appropriate force constant (f) data, barriers can be directly calculated.[1] In this communication we describe an alternative and potentially more general approach to the Franck-Condon barrier problem, based on an experimental application of time-dependent Raman scattering theory.[2,3] The example we have chosen is optical inter-

(1) See, for example: Brunschwig, B. S.; Creutz, C.; Macartney, D. H.; Sham, T.-K.; Sutin, N. *Faraday Dis.* **1983**, *87*, 3360.
(2) (a) Heller, E. J.; Sundberg, R. L.; Tannor, D. *J. Phys. Chem.* **1982**, *86*, 1822. (b) Tannor, D.; Heller, E. J. *J. Chem. Phys.* **1982**, *77*, 202. (c) Lee, S. Y.; Heller, E. J. *J. Chem. Phys.* **1977**, *71*, 4777. (d) Heller, E. J. *Acc. Chem. Res.* **1981**, *14*, 368.
(3) Other applications of the theory are described in the following: (a) Tutt, L.; Zink, J. I. *J. Am. Chem. Soc.* **1986**, *108*, 5830. (b) Zink, J. I.; Tutt, L.; Yang, Y. Y. *ACS Symp. Ser.* **1986**, *307*, 39. (c) Yang, Y. Y.; Zink, J. I. *J. Am. Chem. Soc.* **1985**, *107*, 4799. (d) Tutt, L.; Tannor, D.; Schindler, J.; Heller, E. J.; Zink, J. I. *J. Phys. Chem.* **1983**, *87*, 3017. (e) Tutt, L.; Tannor, D.; Heller, E. J.; Zink, J. I. *Inorg. Chem.* **1982**, *21*, 3858. (f) Zink, J. I. *Coord. Chem. Rev.* **1985**, *64*, 93.

0002-7863/89/1511-1142$01.50/0

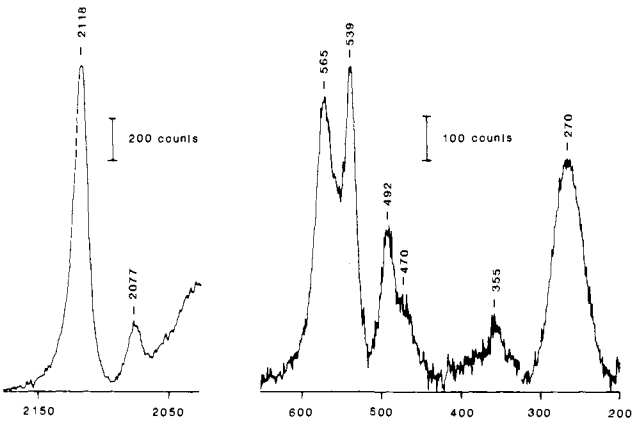

Figure 1. Postresonance Raman spectrum of 40 mM $(CN)_5Ru$-CN-$Ru(NH_3)_5^-$ in H_2O with 514.5-nm excitation.

valence transfer in the unsymmetrical dimer $(NC)_5Ru^{II}$-CN-$Ru^{III}(NH_3)_5^-$ (**1**):[4]

$$(NC)_5Ru^{II}\text{-}CN\text{-}Ru^{III}(NH_3)_5^- \xrightarrow{h\nu} (NC)_5Ru^{III}\text{-}CN\text{-}Ru^{II}(NH_3)_5^{-*} \quad (1)$$

(In a previous paper[5] we have described a simpler case: preresonance-enhanced Raman scattering from the metal-to-ligand charge-transfer transition in $(NH_3)_4Ru(bipyridine)^{2+}$.)

In **1**, an intervalence absorption band of moderate intensity exists with λ_{max} = 684 nm in water. Laser excitation at postresonance (514.5 nm) leads to enhanced Raman scattering as shown in Figure 1.[6] The key feature of the spectrum is that *enhanced scattering is observed from both ends of the mixed-valence ion, based on a single electronic excitation.*[7] For example, an ammine-Ru stretch occurs at 492 cm^{-1}, and C≡N stretches exist at 2077 (weak) and 2118 cm^{-1} (strong). The shift of the strong band to higher energy than found for free $[Ru(CN)_6]^{4-}$,[8b] in addition to the observation of greater effects of solution acidity upon the weak band, leads us to assign the 2118-cm^{-1} mode as the bridging CN stretch.[9] The weak band is then assigned as the terminal CN stretch.

Table I. Structural and Franck–Condon Charge-Transfer Parameters for $(NC)_5Ru$-CN-$Ru(NH_3)_5^-$ from Postresonance Raman (514.5 nm)

band	I_{rel}	$\|\Delta a\|$ (Å)	χ_i' (cm^{-1})	assignment
2118	11	0.046	920	$\nu_{C\text{-}N}$ bridge
2077	3.0	0.012	250	$\nu_{C\text{-}N}$ term
565	1.9	0.035[a]	580	$\nu_{M\text{-}C}$ term } and $\delta_{M\text{-}CN}$
539	2.1	0.078[a]	660	$\nu_{M\text{-}C}$ bridge } and $\delta_{M\text{-}CN}$
492	1	0.039	350	$\nu_{M\text{-}NH_3}$
470	0.54	0.061	190	$\nu_{M\text{-}NH_3}$ (axial)
355	0.36	0.061	170	$\nu_{M\text{-}NC}$
270	1.4		860	$\delta_{H_3N\text{-}M\text{-}NH_3}$

[a] Based on exclusive M–C stretching character in the normal coordinate distortion. (Intervalence enhancement of these bands does suggest an increased M–C stretching character for the unsymmetrical dimer over that found in the monomer.)

Additional bands exist at 565 and 539 cm^{-1}, corresponding to a single band assigned as the ν_7 mode in hexacyano metal monomers.[8] This mode has been shown to contain both M–CN stretching and M—C≡N bending character.[10] On the basis of the shift to lower energy from that found for the monomer, the band at 539 cm^{-1} is assigned as a distortion associated with the bridge, and the higher energy band as a terminal M–CN distortion.[11] The bands at 270- and 470-cm^{-1} shift to lower energy upon ammine deuteration and are assigned as an H_3N–Ru–NH_3 bend[5] and an additional Ru–NH_3 stretch, respectively. The band at 355 cm^{-1} is tentatively assigned as the Ru–NC stretch.

Variations in Raman intensity (I) among the modes (Table I) can be connected in a direct way to unitless normal-coordinate distortions (Δ) by a time-dependent analysis of the scattering phenomenon, as outlined by Heller and co-workers.[2] In the simplest case the relationships are

$$\frac{I_1}{I_2} = \frac{\omega_1^2\Delta_1^2}{\omega_2^2\Delta_2^2} \quad (2)$$

and

$$2\sigma^2 = \sum_k \Delta_k^2(\omega_k/2\pi)^2 \quad (3)$$

where ω is 2π times the vibrational frequency (ν) and $8\sigma^2$ is the square of the absorption bandwidth at 1/e of the height.[12] If a local coordinate approximation is appropriate, the Δ values from eq 2 and 3 can be converted to absolute bond distortions ($|\Delta a|$; Table I) by

$$|\Delta a| = (\Delta^2\hbar/\mu\omega b)^{1/2} \quad (4)$$

where μ is the reduced mass and b is the effective bond degeneracy. The values obtained are reasonably consistent with the few available direct structural assessments for related systems: 1. For $Ru(NH_3)_6^{3+/2+}$ the metal–ammonia bond length change is 0.04 Å by X-ray crystal structure measurements,[1] vs 0.039 Å from Raman measurements with the mixed-valence ion. 2. For $Fe(CN)_6^{3-/4-}$, $\Delta a_{M\text{-}C}$ is −0.026 Å[13] vs ±0.035 Å in **1**,[14,15] if the ν_7

(4) The compound was synthesized as the sodium salt by using the method described in the following: Vogler, A.; Kisslinger, J. *J. Am. Chem. Soc.* **1982**, *104*, 2311.

(5) Doorn, S. K.; Hupp, J. T. *J. Am. Chem. Soc.*, submitted for publication.

(6) Postresonance Raman spectra were obtained from 40 mM aqueous solutions of the complex with 514.5-nm excitation. Resonance Raman spectra were obtained with 647.1-nm excitation of 6 mM solutions of the mixed-valence ion. In each case a bandpass of 9 cm^{-1} was used with 40 mW of excitation light incident on a spinning capillary tube. The low-energy part of the spectrum shown in Figure 1 is a result of subtracting from the original spectrum a broad band centered at 450 cm^{-1} originating from the glass tube.

(7) Intervalence enhancement is demonstrated through a comparison of band intensities from 514.5- and 647.1-nm excitation (with samples prepared in 0.5 M K_2SO_4 using the 981-cm^{-1} sulfate peak as an internal intensity reference). Enhancement factors of 15–20 are found on going from postresonance to resonance excitation. Although in post resonance experiments one must be wary of Raman intensity contributions from transitions to higher lying states,[5] such contributions appear to be unimportant in the present case. From monomer studies[4] the nearest transitions energetically are at 206 nm for $Ru(CN)_6^{4-}$ and 328 nm for $Ru(NH_3)_5Cl^{2+}$. Since neither shows significant extinction in the vicinity of postresonance excitation, it is unlikely that either one contributes importantly to the observed Raman intensities. This conclusion is reinforced by the finding that Δ values obtained with 514.5-nm excitation agree well with those based on excitation at 647.1 nm[12] (i.e., further from high-energy states).

(8) (a) Nakagawa, I.; Shimanouchi, T. *Spectrochim. Acta* **1962**, *18*, 101. (b) Griffith, W. P.; Turner, G. T. *J. Chem. Soc. A* **1970**, 858. (c) Hawkins, N. J.; Mattraw, H. C.; Sabol, W. W.; Carpenter, D. R. *J. Chem. Phys.* **1955**, *23*, 2422.

(9) Bridging occurs via electron withdrawal from the lowest CN σ^* orbital, effectively increasing the CN bond order and stretching frequency. See, for example: (a) Shriver, D. F.; Shriver, S. A.; Anderson, S. E. *Inorg. Chem.* **1965**, *4*, 725. (b) Hester, R. E.; Nour, E. M. *J. Chem. Soc., Dalton Trans.* **1981**, 939. (c) Allen, C. S.; Van Duyne, R. P. *J. Am. Chem. Soc.* **1981**, *103*, 7497.

(10) Jones, L. H.; Memering, M. N.; Swanson, B. I. *J. Chem. Phys.* **1971**, *54*, 4666.

(11) Electron withdrawal to form the bridging bond presumably reduces the ability to σ bond through the carbon atom, thereby resulting in a decreased force constant for the vibration.

(12) Equations 2 and 3 are correctly applied only in the limit of "short time dynamics".[2] This limit can be reached either by performing the experiment far from resonance or by choosing a system with a sufficiently large number of normal coordinate distortions. In our case the first condition is met by excitation at 514 nm. Scattering experiments close to resonance (647 nm) indicate that the second condition is also nearly fulfilled but that some preferential enhancement of the 492- and 355-cm^{-1} modes occurs. All subsequent analyses were therefore confined to postresonance conditions.

(13) Swanson, B. I.; Hamburg, S. I.; Ryan, R. R. *Inorg. Chem.* **1974**, *13*, 1685.

(14) The Raman scattering technique indicates the magnitude, but not the sign, of the distortion. See, however: Myers, A. B.; Mathies, R. A. In *Biological Applications of Raman Spectroscopy*; Spiro, T. G., Ed.; John Wiley & Sons: New York, Vol. 2.

mode is attributed completely to bond compression. 3. Again for $Fe(CN)_6^{3-/4-}$, Δa_{CN} is 0.01 ± 0.01 Å[13] vs 0.012 Å for **1**. It is worth noting that the C≡N distortion occurs at the limit of precision in the X-ray measurements,[13] but that it is rather easily detected and quantitated by postresonance Raman. We have remarked elsewhere, however, that the Raman-based Δa values could be in error by as much as +20% due to spin-orbit coupling and solvent contributions to σ^2 in eq 3.[5]

From the normal coordinate or bond distortion data, individual contributions (χ_i'; Table I) to the vibrational reorganization energy can be calculated:

$$\chi_i' = (1/2)b(\Delta a)^2 f = (1/2)\Delta^2 \nu \qquad (5)$$

From the table the following points are worth noting: 1. Both ends of the mixed-valence ion participate in vibrational trapping. 2. Nearly half of the trapping or reorganization energy comes from modes assigned to the bridging ligand. 3. Local modes remote from the metal center (i.e., C≡N stretches) can contribute measurably to the Franck-Condon energy. 4. The low-energy metal-ammine bend (which is generally overlooked) is as significant as the higher energy Ru-NH_3 stretch. It is important to realize that point 2, in particular, would be difficult to establish by any conventional X-ray structural method and that the Raman method appears, at present, to provide the only quantitative route to such information.

We intend to report shortly on a more general study of $(NC)_5M$-CN-$M'(NH_3)_5^-$ systems where M = Fe, Ru, Os and M' = Ru, Os. We also have carried out preliminary studies of symmetrical mixed-valence ions by using near infrared laser excitation. Our current effort is directed toward ion-paired metal monomers which exhibit outer-sphere charge-transfer transitions.

Acknowledgment. This work was supported by the U.S. Department of Energy (Grant No. DE-FGO2-87KR13808). The Raman facility is part of the Northwestern University Materials Research Center and is supported by a grant from NSF (DMR-8520280). We thank Dr. Basil Swanson and Professor Du Shriver for helpful discussions regarding the Raman spectral assignments.

(15) The comparison to $Fe(CN)_6^{3-/4-}$ may be less than completely appropriate since the extent of backbonding certainly will differ for M = Ru vs M = Fe. Unfortunately, independent structural data for $Ru(CN)_6^{3-/4-}$ are lacking.

Peptide Bond Formation at the Micellar Interface†

D. Ranganathan,* G. P. Singh, and S. Ranganathan

Department of Chemistry, Indian Institute of Technology, Kanpur 208016, India

Received May 23, 1988
Revised Manuscript Received November 19, 1988

The highly preorganized reverse micellar system harboring water pools—formed by adding 100 mM AOT (bis(2-ethylhexyl)sodium sulfosuccinate) to isooctane containing 2% water—appeared to us as an ideal take off point to study the possibility of selective peptide bond formation.

Extensive work[1] has shown that such a micellar system can be best represented as shown in Figure 1a.

It was conjectured that a prerequisite for the peptide bond formation under nonenzymatic conditions would require the introduction of a cosurfactant harboring a carbodiimide moiety.

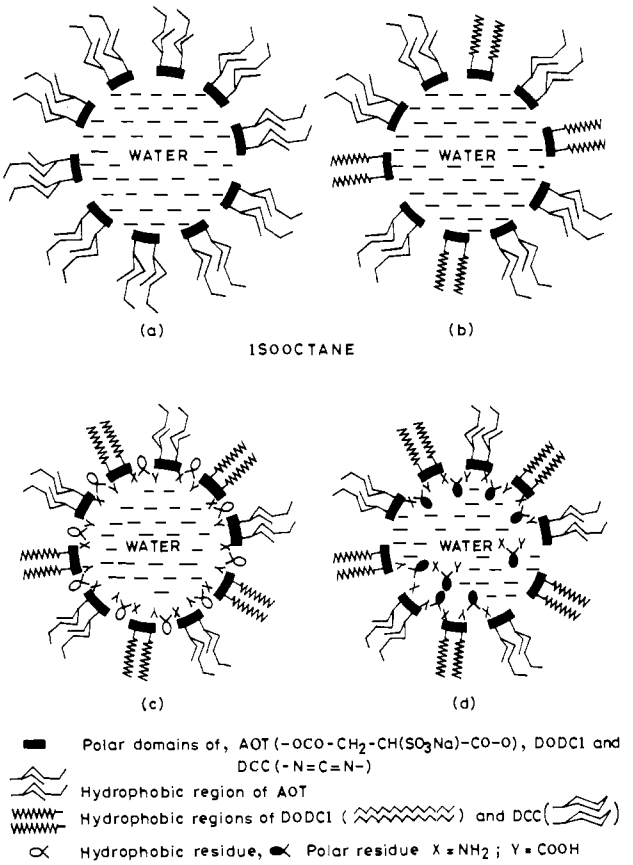

Figure 1. Schematic illustration of possible stages in the formation of peptide bond at the interface of the reverse micelle with hydrophobic and polar amino acids: (a) The highly organized reverse micellar system harboring water pools—formed by addition of 10 mM AOT to 100 mL of isooctane containing 2 mL of water; (b) The alignment of either DCC (structurally similar to AOT) or DODCI (possessing long hydrophobic tails) as cosurfactant; (c) The arrangement of hydrophobic amino acids at the micellar surface and their diffusion to the interface. Both properties promote the formation of the peptide bond; (d) The distribution of polar amino acids in the water pool. The peptide formation here is linked to the concentration in the immediate micellar environment.

Dicyclohexylcarbodiimide (DCC)[2] whose hydrophobic region bears a striking resemblance to that of AOT (Figure 1a) and the novel reagent, dioctadecylcarbodiimide (DODCI), possessing extended hydrophobic tail segments,[3] were considered appropriate for the study. It was envisaged that the introduction of either DCC or DODCI into the reverse micellar system would lead to an ordered arrangement as shown in Figure 1b. This model appeared to us to be sufficiently attractive to study the peptide bond formation from amino acids possessing hydrophobic and polar residues.

The hydrophobic amino acid residues can be expected to align at the micellar interface in proximate relationship to DODCI/DCC (Figure 1c), thus facilitating the formation of the activated ester, the key step in the formation of the peptide bond. On the other hand, amino acids carrying polar side chains would be distributed in the water pool, and therefore peptide bond formation here would be governed by the extent of their interaction with the condensing agents (DCC/DODCI) at the micellar interface (Figure 1d). Thus, based on models presented in Figure 1c and 1d, peptide bonds involving hydrophobic residues would be more favored than those with polar ones.

† This work is respectfully dedicated to Professor Sir D. H. R. Barton on the occasion of his 70th birthday.

(1) *Reverse Micelles*; Luisi, P. L., Straub, B. E., Eds.; Plenum Press: New York, 1984. Luisi, P. L. *Angew. Chem., Int. Ed. Engl.* **1985**, *24*, 439. Luisi, P. L.; Magid, L. J. *CRC Critical Rev. Biochem.* **1986**, *20*, 409. Luisi, P. L., Steinmann-Hofmann, B. *Methods Enzymol.* **1987**, *136*, 188.

(2) We are most grateful to a referee for this valuable suggestion.

(3) DODCI, mp 48 °C, was prepared in 77% overall yield by the condensation of octadecylamine (20 mM) with CS_2 (10 mM) in dry EtOH to thiourea followed by HgO oxidation in CS_2 and Na_2SO_4 (anhydrous). DODCI is a useful condensing agent for peptide synthesis.

0002-7863/89/1511-1144$01.50/0